THIS REPORT HAS BEEN DELIMITED
AND CLEARED FOR PUBLIC RELEASE
UNDER DOD DIRECTIVE 5200.20 AND
NO RESTRICTIONS ARE IMPOSED UPON
ITS USE AND DISCLOSURE.

DISTRIBUTION STATEMENT A

APPROVED FOR PUBLIC RELEASE;
DISTRIBUTION UNLIMITED.

UNCLASSIFIED

AD 125051

Armed Services Technical Information Agency

Reproduced by

DOCUMENT SERVICE CENTER

KNOTT BUILDING, DAYTON, 2, OHIO

This document is the property of the United States Government. It is furnished for the duration of the contract and shall be returned when no longer required, or upon recall by ASTIA to the following address: Armed Services Technical Information Agency, Document Service Center, Knott Building, Dayton 2, Ohio.

NOTICE: WHEN GOVERNMENT OR OTHER DRAWINGS, SPECIFICATIONS OR OTHER DATA ARE USED FOR ANY PURPOSE OTHER THAN IN CONNECTION WITH A DEFINITELY RELATED GOVERNMENT PROCUREMENT OPERATION, THE U. S. GOVERNMENT THEREBY INCURS NO RESPONSIBILITY, NOR ANY OBLIGATION WHATSOEVER; AND THE FACT THAT THE GOVERNMENT MAY HAVE FORMULATED, FURNISHED, OR IN ANY WAY SUPPLIED THE SAID DRAWINGS, SPECIFICATIONS, OR OTHER DATA IS NOT TO BE REGARDED BY IMPLICATION OR OTHERWISE AS IN ANY MANNER LICENSING THE HOLDER OR ANY OTHER PERSON OR CORPORATION, OR CONVEYING ANY RIGHTS OR PERMISSION TO MANUFACTURE, USE OR SELL ANY PATENTED INVENTION THAT MAY IN ANY WAY BE RELATED THERETO.

UNCLASSIFIED

AD No. 125051
ASTIA FILE COPY

THE DAVID W. TAYLOR MODEL BASIN

UNITED STATES NAVY

FC

PLASTIC DEFORMATION OF A THIN CIRCULAR PLATE UNDER PRESSURE

BY A. N. GLEYZAL, PH. D

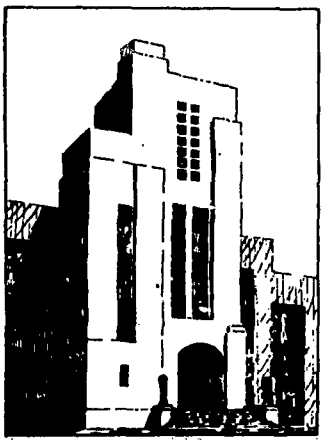

MARCH 1946

REPORT 532

REPORT 532

PLASTIC DEFORMATION OF A THIN CIRCULAR PLATE UNDER PRESSURE

BY A.N. GLEYZAL, Ph. D.

MARCH 1947

PLASTIC DEFORMATION OF A THIN CIRCULAR PLATE UNDER PRESSURE

ABSTRACT

In this report a numerical solution is given of a set of equations consisting essentially of three plasticity laws, two strain-displacement laws, and two equilibrium laws, which describe the action of a clamped, thin, circular plate as it yields plastically when pressure is applied to one side. The stresses, strains, thickness variation, and deflections for any thin circular plate of a given material may be computed by the numerical integration of the equilibrium conditions, the geometric conditions relating displacements and strains, and the stress-strain laws. The solution may be reduced to the solution of a second-order differential equation with the radial distance r as independent variable. The solution depends upon an experimentally determined function, $\tau(\gamma)$, which describes the stress-strain properties of the material, and upon three parameters, the pressure p, the original thickness h_0, and the radius a of the clamping ring. It is found that for a given material, a family of curves with pa/h_0 as a parameter serves to predict the solution for any thin circular plate of the same material.

This analysis has been carried out for a particular function $\tau(\gamma)$ based on results of a tensile test made on a specimen of medium steel. Graphs of theoretically and experimentally determined values of deflection, radial and circumferential strains, radial and circumferential stresses, and thickness corresponding to various pressures are presented which apply to all plates made of the same steel as this specimen.

INTRODUCTION

The plastic action of a circular plate under static pressures great enough to cause rupture is of interest to the David Taylor Model Basin in its program of study of damage to ships caused by underwater explosions. The clamped circular plate is a simple model regarded as analogous in some respects to one of the plate panels in a ship. The static pressure applied to the circular plate is in the ship replaced by the pressure due to an underwater explosion.

When sufficient pressure is applied to one side of a circular steel plate clamped around its edge, the plate is deformed into an approximately spherical dome or cap. If the clamping ring has a curved edge as in Figure 1, the rim of the cap is tangent to the curved edge. As the plate deforms the metal flows so that the plate thins markedly at its center and only slightly near the rim. A point P on the initially flat plate moves along

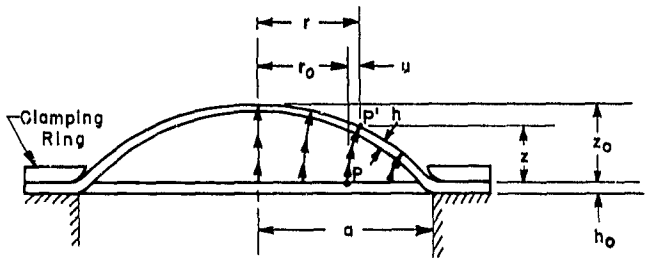

Figure 1 - Diagram Showing a Thin Circular Plate as It Deforms Plastically under Pressure

a curve such as PP′ to P′. For a given deflection of the diaphragm the radial displacement u is zero at the center by reason of symmetry, reaches a maximum somewhere between the center and edge of the plate, and drops to zero again at the rim.

The behavior of a circular plate in the elastic range has been considered by Hencky (1)* and by S. Way (2). In Hencky's solution bending stresses are neglected. Way has taken both bending and stretching into account. Since the present analysis is concerned with thin plates, the bending stresses are neglected here also. This analysis differs from Hencky's in that it is concerned primarily with the plastic range up to rupture. The results presented here are valid for values of z_0/a ranging from about 0.03 up to about 0.30, where z_0 is the central deflection. For values of z_0/a corresponding to elastic deflection, that is, when z_0/a is less than 0.03, the results nevertheless have some validity since, as will be shown, the plasticity laws chosen are identical, for small strains, with the elasticity laws provided Poisson's ratio is taken as 0.5.

The purpose of the present report is to show how certain plasticity laws, three in number, which involve an experimentally-obtained octahedral stress-strain curve $\tau(\gamma)$, may be used to compute stresses, strains, and displacements in a thin circular plate when merely the dimensions of the plate, the pressure applied, and the true tensile stress-strain curve up to rupture of a specimen of the material are given. The present problem has its parallel in elasticity theory, but the methods employed in this report are almost necessarily graphical and numerical due to the nonlinear character of the stress-strain laws of plasticity. Emphasis will be placed on finding a feasible approximate method to solve the general plasticity problem of the clamped, thin, circular plate rather than on attaining a close check between experiment and theory. Improvements in the theory which would yield numerical results in closer agreement with experimental results are suggested at the end of the report.

---

* Numbers in parentheses indicate references on page 30 of this report.

BASIC ASSUMPTIONS

The calculation of stresses, strains, and displacements involves solving simultaneously two equations which express the conditions of equilibrium, two geometrical relationships of strain and displacement, and three plasticity laws which relate stress with strain in the material. In the theory the plate is assumed to be clamped by a rigid ring with a sharp inner edge; bending moments are assumed negligible since the plate is thin. Consequently, the surface of the loaded plate meets the plane of the rim at a finite angle. The methods and formulas used in the calculations, excepting perhaps the plasticity laws, are exact but for the omission of second-order terms. Hence the validity of the results obtained hinges largely on the validity of the three plasticity laws which are assumed. Of these laws, one, which expresses constancy of volume of the material, has been verified experimentally with a high degree of accuracy for certain metals. Agreement with experiment is reasonably good for the other two laws.

DEFINITION OF STRAIN

Although there is no question in the literature as to the definition of stress and the stress tensor, there is some choice in the definition of strain. The *conventional strain* $\epsilon = \frac{l - l_0}{l_0}$, where l and l_0 are the final and the initial lengths respectively, may be considered basic and other definitions of strain can be made in terms of it. The *logarithmic strain*, for example, designated as ϵ', has been defined by Ludwik (3) as

$$\epsilon' = \int_0^{\epsilon} \frac{d\epsilon}{1 + \epsilon} = \log(1 + \epsilon)$$

where ϵ is the conventional strain. Another definition based on the quadratic form for the square of the differential of arc-length, one which guarantees the existence of a strain tensor, has been considered by Synge and Chien (4). For the sake of simplicity, and because the equations to be employed are necessarily approximate themselves, *strain* will be taken to mean *conventional strain* in this report.

STRESS-STRAIN EQUATIONS OF PLASTICITY

The plasticity laws stated in the following were given by Nadai (5) (6); they are based on the work of a number of writers, among whom may be mentioned von Mises (7) and Mohr (8). White (9) has applied them to a theoretical investigation of circular diaphragms under pressure. They have been tested experimentally by Schmidt (10), Taylor and Quinney, Ros and Eichinger,

Nadai and Lode, and others. Nadai (6) (11) has written accounts of, and given references for the theoretical and experimental work of these and other writers. Davis (12) (13) has made a series of tests on cylindrical tubes to verify these plasticity laws for copper and medium steel.

The stress-strain relations of plasticity which are assumed in this report are

$$\epsilon_1 + \epsilon_2 + \epsilon_3 = 0 \qquad [1a]$$

$$\frac{\epsilon_1 - \epsilon_2}{\sigma_1 - \sigma_2} = \frac{\epsilon_2 - \epsilon_3}{\sigma_2 - \sigma_3} = \frac{\epsilon_3 - \epsilon_1}{\sigma_3 - \sigma_1} = \frac{1}{\lambda} \qquad [1b]$$

$$\tau = \tau(\gamma) \qquad [1c]$$

where

$$\tau = \frac{1}{3}\left[(\sigma_1 - \sigma_2)^2 + (\sigma_2 - \sigma_3)^2 + (\sigma_3 - \sigma_1)^2\right]^{\frac{1}{2}} \qquad [2a]$$

$$\gamma = \frac{2}{3}\left[(\epsilon_1 - \epsilon_2)^2 + (\epsilon_2 - \epsilon_3)^2 + (\epsilon_3 - \epsilon_1)^2\right]^{\frac{1}{2}} \qquad [2b]$$

and, as will be shown,

$$\lambda = 2\frac{\tau}{\gamma} \qquad [3]$$

In these equations ϵ_1, ϵ_2, and ϵ_3 are the principal strains and σ_1, σ_2, and σ_3 are the principal stresses. The quantities γ and τ have been shown by Nadai (11) to be, respectively, the shear strain and the shear stress in an octahedral plane, a plane whose normal makes equal angles with the three principal directions of strain or stress.

Equation [1a] implies that, to a first order, volumes remain constant. Equation [1b] is usually associated with the assumption that at any one point the principal axes of stress coincide with the principal axes of strain. It may be shown that the latter condition is satisfied for a thin circular plate under pressure. The quantity λ depends on the material as well as on the state of stress and strain at each point. Equation [1c] implies that $\tau(\gamma)$ is the same function of γ for all states of stress and strain in a material. Thus, if γ has the same numerical value in two states, then by this formula τ will have the same value in the two states. Hence $\tau(\gamma)$ may be considered to characterize the material with respect to its stress-strain properties. It can be determined by a tensile test on the material, or by tests on plates deformed under pressure, using formulas given later in this report.

It may be noted that, since $\epsilon_3 = -(\epsilon_1 + \epsilon_2)$,

$$\gamma = 2\sqrt{\frac{2}{3}}\sqrt{\epsilon_1^2 + \epsilon_1\epsilon_2 + \epsilon_2^2} \qquad [4]$$

Equations [1] are three independent relations which connect the six variables ϵ_1, ϵ_2, ϵ_3 and σ_1, σ_2, σ_3. They correspond to the three stress-strain laws of elasticity, and, in fact, may be put into a form which corresponds closely to these laws. Combining Equation [1b] with Equations [2a] and [2b], it is easily seen that

$$\lambda = 2\frac{\tau}{\gamma}$$

and as a consequence of Equation [1c] the ratio λ is seen to be a definite function of γ also. The principal shear stresses may therefore be expressed in terms of shear strains by the formulas

$$\left.\begin{aligned} \frac{\sigma_1 - \sigma_2}{2} &= \frac{\tau(\gamma)}{\gamma}(\epsilon_1 - \epsilon_2) \\ \frac{\sigma_2 - \sigma_3}{2} &= \frac{\tau(\gamma)}{\gamma}(\epsilon_2 - \epsilon_3) \\ \frac{\sigma_3 - \sigma_1}{2} &= \frac{\tau(\gamma)}{\gamma}(\epsilon_3 - \epsilon_1) \end{aligned}\right\} \qquad [5]$$

These equations are equivalent to

$$\left.\begin{aligned} \sigma_1 &= 2\frac{\tau(\gamma)}{\gamma}\epsilon_1 + \Sigma \\ \sigma_2 &= 2\frac{\tau(\gamma)}{\gamma}\epsilon_2 + \Sigma \\ \sigma_3 &= 2\frac{\tau(\gamma)}{\gamma}\epsilon_3 + \Sigma \end{aligned}\right\} \qquad [6]$$

where $\Sigma = \frac{1}{3}(\sigma_1 + \sigma_2 + \sigma_3)$ is the mean normal stress as may be seen by equating the sum of the three left-hand members of Equations [6] to the sum of the three right-hand members of these equations and making use of Equation [1a]. The physical implication is that a hydrostatic stress may be added to existing stresses without changing the strains.

Equations [6] solved for strains in terms of stresses give

$$\left.\begin{aligned} \epsilon_1 &= \frac{1}{3}\frac{\gamma(\tau)}{\tau}\left[\sigma_1 - \frac{1}{2}(\sigma_2 + \sigma_3)\right] \\ \epsilon_2 &= \frac{1}{3}\frac{\gamma(\tau)}{\tau}\left[\sigma_2 - \frac{1}{2}(\sigma_1 + \sigma_3)\right] \\ \epsilon_3 &= \frac{1}{3}\frac{\gamma(\tau)}{\tau}\left[\sigma_3 - \frac{1}{2}(\sigma_1 + \sigma_2)\right] \end{aligned}\right\} \qquad [7]$$

where $\gamma(\tau)$ is the function which is inverse to $\tau(\gamma)$. These expressions are of the same form as the laws of elasticity; the factor $\gamma(\tau)/3\tau$ replaces $1/E$ and the factor 1/2 replaces ν, where ν denotes Poisson's ratio.

DETERMINATION OF $\tau(\gamma)$ FROM A TENSILE TEST

The function $\tau(\gamma)$ may be expressed in terms of quantities measured in a tensile test of the material. This is true because in such a test, if the three principal stresses are denoted by

$$\sigma_1 = \sigma_1, \quad \sigma_2 = 0, \quad \sigma_3 = 0$$

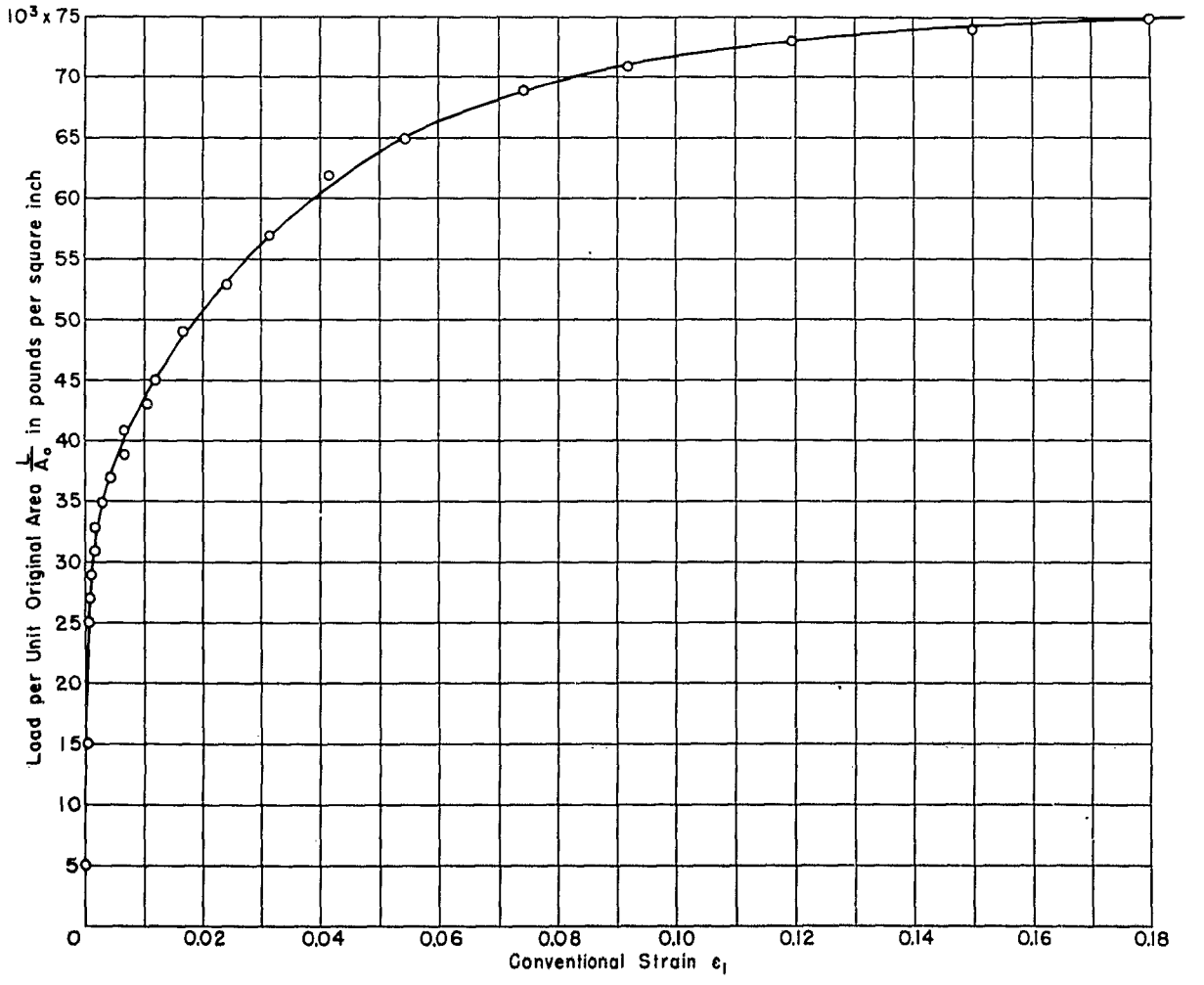

Figure 2 - A Load-Strain Curve for a Medium-Steel Tensile Specimen

This load-strain curve was obtained from a round medium-steel specimen, 0.505 inch in diameter, made from the same sheet of medium steel as the experimental plate described in this report. This curve is considered to "describe" the material; it was used as the basis for all computations for the theoretical prediction of the action of a thin plate of this material.

and the three principal strains by

$$\epsilon_1 = \epsilon_1, \quad \epsilon_2 = -\frac{1}{2}\epsilon_1, \quad \epsilon_3 = -\frac{1}{2}\epsilon_1$$

then, from Equations [2a] and [2b]

$$\tau = \frac{\sqrt{2}}{3}\sigma_1 \qquad [8a]$$

$$\gamma = \sqrt{2}\,\epsilon_1 \qquad [8b]$$

Since the load L and the strain ϵ_1 are the quantities usually measured in a tensile test, it is useful to write the equation for σ_1 in

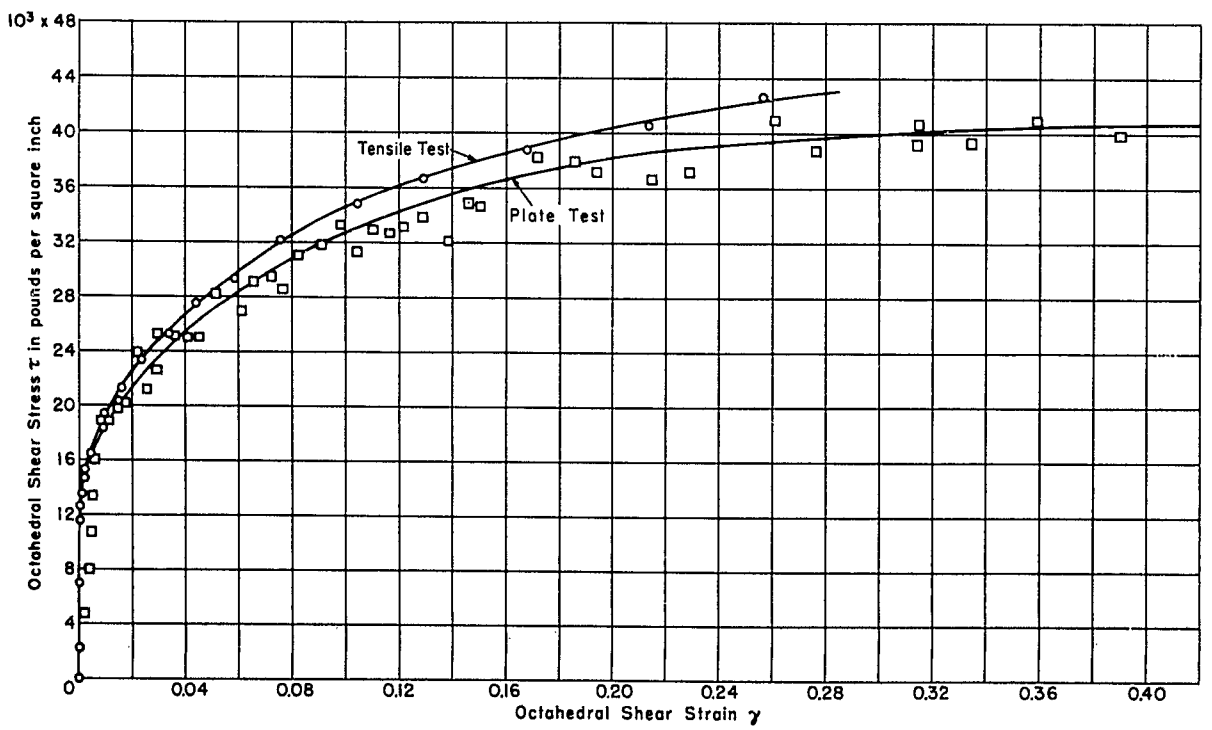

Figure 3 - Octahedral Shear Stress Plotted against Octahedral Shear Strain

The calculations of this report were based on the $\tau(\gamma)$ curve shown here. The load-strain curve from which $\tau(\gamma)$ was computed is shown in Figure 2. The $\tau(\gamma)$ curve calculated from measurements at the center of an experimental plate of the same material, medium steel, is shown for comparison. The difference between the two curves accounts in large part for the difference between computed and experimental values of deflection in Figure 13 on page 28.

The quantities τ and γ for the tensile test were computed by Equations [8] and [9]. For the plate test they were computed by Equations [11], [16], [17], [18], and [19] by use of measured values of pressure, deflection, and strains. For strains in the region of necking of a tensile specimen, $\tau(\gamma)$ should be determined from measurements of instantaneous load and minimum cross-sectional area A of the specimen. In this region σ_1 should be taken as L/A and ϵ_1 as $(A_0 - A)/A$.

terms of them. In a tensile test the cross-sectional area is

$$A = A_0(1 + \epsilon_2)(1 + \epsilon_3)$$

where A_0 is the original cross-sectional area. It follows that

$$\sigma_1 = \frac{L}{A} = \frac{L}{A_0} \frac{1}{\left(1 - \frac{1}{2}\epsilon_1\right)^2}$$

Therefore, approximately,

$$\sigma_1 = \frac{L}{A_0}(1 + \epsilon_1) \qquad [9]$$

The curve $\tau(\gamma)$ of Figure 3, which shows the relation between octahedral shear stress and octahedral shear strain, was computed from the load-strain curve $L(\epsilon_1)$ of Figure 2 by the use of Equations [8] and [9]. For comparison, the $\tau(\gamma)$ curve determined by measurements on an experimental plate of the same material under pressure is included in Figure 3. The extent to which the two curves agree is a measure of the validity of the plasticity laws assumed in this report. The difference between the two curves accounts for a large portion of the difference between the experimental and the theoretical results presented herein.

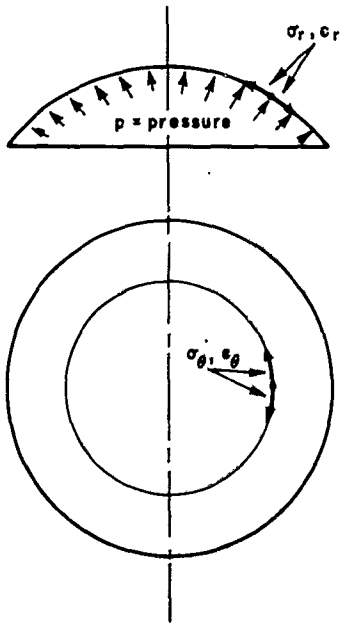

Figure 4 - The Principal Stresses and Strains in a Circular Plate under Pressure

STRESS-STRAIN LAWS FOR A THIN PLATE

As a thin circular plate clamped at the rim deflects under pressure, symmetry requires that one of the principal stresses be the stress σ_r in the radial direction and another be the stress σ_θ in the circumferential direction, as in Figure 4. Similarly one of the principal strains is ϵ_r, the strain in the radial direction, and another is ϵ_θ, the strain in the circumferential direction. If σ_1 and σ_2 of Equations [6] are interpreted to be σ_r and σ_θ respectively, then σ_3 is the stress in the direction perpendicular to the plate at the point. This stress is of the order of the pressure on the plate and hence is of relatively negligible

magnitude. If σ_3 is set equal to zero and the relation $\epsilon_3 = -(\epsilon_1 + \epsilon_2)$ is used in Equation [5], the result will be

$$\sigma_r = 2\frac{\tau(\gamma)}{\gamma}(2\epsilon_r + \epsilon_\theta) \qquad [10a]$$

$$\sigma_\theta = 2\frac{\tau(\gamma)}{\gamma}(2\epsilon_\theta + \epsilon_r) \qquad [10b]$$

where now, by Equation [4],

$$\gamma = 2\sqrt{\frac{2}{3}}\sqrt{\epsilon_r^2 + \epsilon_r\epsilon_\theta + \epsilon_\theta^2} \qquad [11]$$

Also, for biaxial stresses Equation [2a] implies that

$$\tau = \frac{\sqrt{2}}{3}\sqrt{\sigma_r^2 - \sigma_r\sigma_\theta + \sigma_\theta^2}$$

The foregoing relations may be called the plastic stress-strain equations for a plate under biaxial stress.

STRAINS IN TERMS OF DISPLACEMENTS AND DEFLECTIONS

Suppose a flat circular plate is deflected to a radially symmetrical shape as shown in Figure 1. The axis of symmetry may be taken as the z-axis

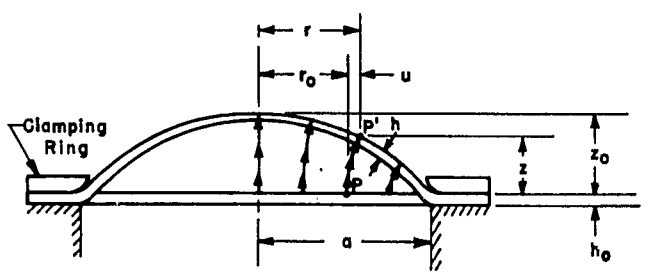

Figure 1 - Diagram Showing a Thin Circular Plate as It Deforms Plastically under Pressure

in a set of cylindrical coordinates r, θ, z. As the plate deforms, a point P on the plate moves along a path such as PP'. Let u denote the radial displacement for the point P'. If z is the deflection of this point then the point P of coordinates r_0, θ_0, 0 on the undeformed plate has the final coordinates r, θ, z. By symmetry $\theta = \theta_0$ and the square of the arc length

$$ds_0^2 = dr_0^2 + r_0^2 d\theta_0^2$$

of an element on the undeformed plate has as its final arc length

$$ds^2 = dr^2 + r^2 d\theta^2 + dz^2$$

The strain for this element is therefore

$$\frac{ds - ds_0}{ds_0} = \frac{ds}{ds_0} - 1 = \sqrt{\frac{dr^2 + r^2 d\theta^2 + dz^2}{dr_0^2 + r_0^2 d\theta_0^2}} - 1 \qquad [12]$$

If $d\theta = d\theta_0$ is set equal to zero in this expression, the radial strain is found to be

$$\epsilon_r = \sqrt{\frac{dr^2 + dz^2}{dr_0^2}} - 1$$

or,

$$\epsilon_r = \frac{\sqrt{1 + \left(\frac{dz}{dr}\right)^2}}{\frac{dr_0}{dr}} - 1$$

Therefore, since $r_0 = r - u$,

$$\epsilon_r = \frac{\sqrt{1 + \left(\frac{dz}{dr}\right)^2}}{1 - \frac{du}{dr}} - 1 \qquad [13]$$

If du/dr and dz/dr are small quantities, Equation [13] may be written in the approximate form

$$\epsilon_r = \frac{du}{dr} + \frac{1}{2}\left(\frac{dz}{dr}\right)^2 \qquad [14]$$

By setting $dr_0 = 0$, and $dr = dr_0 + du = du$ in Equation [12] the circumferential strain is found to be

$$\epsilon_\theta = \sqrt{\frac{du^2 + r^2 d\theta^2 + dz^2}{r_0^2 d\theta_0^2}} - 1$$

Therefore, since $\theta = \theta_0$,

$$\epsilon_\theta = \frac{1}{r_0}\sqrt{r^2 + \left(\frac{du}{d\theta}\right)^2 + \left(\frac{dz}{d\theta}\right)^2} - 1$$

Because of radial symmetry, $du/d\theta = 0$ and $dz/d\theta = 0$. Hence

$$\epsilon_\theta = \frac{r}{r_0} - 1$$

or

$$\epsilon_\theta = \frac{u}{r_0}$$

In terms of the final radius r,

$$\epsilon_\theta = \frac{u}{r - u}$$

Since u is small relative to r, we write for the purposes of this report simply

$$\epsilon_\theta = \frac{u}{r} \qquad [15]$$

Equations [14] and [15] for strains in terms of displacements are the familiar ones for the circular plate in elasticity theory.

THICKNESS IN TERMS OF STRAINS

Let ϵ_z denote the strain in the direction normal to the surface of the plate. Then by Equation [1a]

$$\epsilon_z = -(\epsilon_r + \epsilon_\theta)$$

If h_0 is the initial thickness and h the thickness of the plate when deformed, then, by definition,

$$\epsilon_z = \frac{h - h_0}{h_0}$$

It follows that

$$h = h_0(1 - \epsilon_r - \epsilon_\theta) \qquad [16]$$

EQUILIBRIUM CONDITIONS

Suppose that under a pressure p the deflection function for a circular plate is $z(r)$. The force resulting from the pressure on a cap of radius r, Figure 5, in the direction of the z-axis is $\pi r^2 p$. This force is balanced by a vertical force* due to the radial tension t_r in the plate:

$$2\pi r \frac{\frac{dz}{dr}}{\sqrt{1 + \left(\frac{dz}{dr}\right)^2}} t_r$$

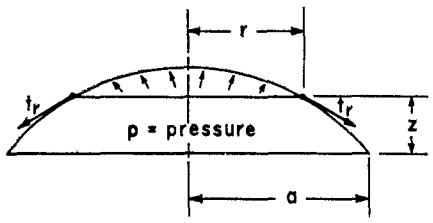

Figure 5 - Forces on a Spherical Cap

* The sign of the square root which appears in this expression is chosen so that the expression is positive.

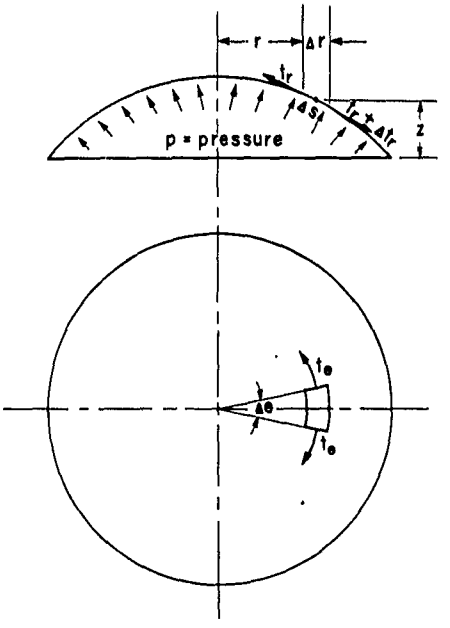

Figure 6 - Forces on an Element of a Spherical Cap

When these forces on the cap are equated, there results

$$\pi r^2 p = 2\pi r \frac{\frac{dz}{dr}}{\sqrt{1 + \left(\frac{dz}{dr}\right)^2}} t_r$$

or

$$t_r = \frac{1}{2} p \frac{r}{\frac{dz}{dr}} \sqrt{1 + \left(\frac{dz}{dr}\right)^2} \qquad [17]$$

Consider now the element defined by $\Delta\theta$ and Δs as in Figure 6. The resultant force on the element due to the circumferential tensions t_θ at each end, as shown in Figure 6, is approximately $t_\theta \Delta\theta \Delta s$. This force acts radially inward in a plane parallel to the original plane of the plate. The component of this force in the direction of the radial tension is approximately $t_\theta \Delta\theta \Delta s \frac{\Delta r}{\Delta s} = t_\theta \Delta\theta \Delta r$. The total force on the element, due to the radial tension t_r, is approximately $(r + \Delta r)\Delta\theta(t_r + \Delta t_r) - r\Delta\theta t_r$. No component due to pressure exists in the t_r direction. Hence, if the forces in the t_r direction are equated, there results the approximate equation

$$t_\theta \Delta\theta \Delta r = (r + \Delta r)\Delta\theta(t_r + \Delta t_r) - r\Delta\theta t_r$$

or

$$t_\theta = \frac{(r + \Delta r)(t_r + \Delta t_r) - r t_r}{\Delta r}$$

If we let Δr approach zero, we obtain the exact equation

$$t_\theta = \frac{d}{dr}(r t_r) = t_r + r \frac{d}{dr}(t_r) \qquad [18]$$

or

$$t_\theta = p \frac{r}{\frac{dz}{dr}} \sqrt{1 + \left(\frac{dz}{dr}\right)^2} - \frac{1}{2} p \frac{r^2}{\left(\frac{dz}{dr}\right)^2} \frac{\frac{d^2z}{dr^2}}{\sqrt{1 + \left(\frac{dz}{dr}\right)^2}}$$

Thus, both t_r and t_θ may be expressed in terms of the deflection function $z(r)$ and the pressure p. The stresses σ_θ and σ_r may be expressed in

terms of t_r, t_θ, and the thickness h as follows,

$$\sigma_r = \frac{t_r}{h} \qquad [19a]$$

$$\sigma_\theta = \frac{t_\theta}{h} \qquad [19b]$$

By combining Equations [19] with Equations [14], [15], [16], [17], and [18], it is seen that, if the displacements u and z of every point on the plate and the pressure p are known, the stresses may be computed.

SOLUTION OF EQUATIONS FOR PLASTIC DEFORMATION OF A CIRCULAR PLATE

From the equations derived in the foregoing, the following independent set of equations may be chosen to describe the action of the thin circular plate under pressure:

$$t_r = \frac{1}{2} p \frac{r}{\frac{dz}{dr}} \sqrt{1 + \left(\frac{dz}{dr}\right)^2} \qquad [17]$$

$$t_\theta = t_r + r \frac{d}{dr}(t_r) \qquad [18]$$

$$\sigma_r = 2 \frac{\tau(\gamma)}{\gamma} (2\epsilon_r + \epsilon_\theta) \qquad [10a]$$

$$\sigma_\theta = 2 \frac{\tau(\gamma)}{\gamma} (2\epsilon_\theta + \epsilon_r) \qquad [10b]$$

$$\epsilon_r = \frac{du}{dr} + \frac{1}{2}\left(\frac{dz}{dr}\right)^2 \qquad [14]$$

$$\epsilon_\theta = \frac{u}{r} \qquad [15]$$

$$h = h_0(1 - \epsilon_r - \epsilon_\theta) \qquad [16]$$

$$\sigma_r = \frac{t_r}{h} \qquad [19a]$$

$$\sigma_\theta = \frac{t_\theta}{h} \qquad [19b]$$

$$\gamma = 2\sqrt{\frac{2}{3}} \sqrt{(\epsilon_r^2 + \epsilon_r \epsilon_\theta + \epsilon_\theta^2)} \qquad [11]$$

These equations are ten independent relations in the ten variables t_r, t_θ, z, u, σ_r, σ_θ, ϵ_r, ϵ_θ, γ, and h, containing the arbitrary parameters p and h_0 and the function $\tau(\gamma)$, which describes the material with respect to its plastic stress-strain properties. The equations will now be transformed into others suited to solution by numerical integration.

Equations [14] and [15] imply

$$\epsilon_r = \frac{d}{dr}(r\epsilon_\theta) + \frac{1}{2}\left(\frac{dz}{dr}\right)^2$$

or,

$$\epsilon_r = \epsilon_\theta + r\frac{d\epsilon_\theta}{dr} + \frac{1}{2}\left(\frac{dz}{dr}\right)^2 \qquad [20]$$

By solving for $\frac{dz}{dr}$ in Equation [17], we find that

$$\frac{dz}{dr} = \frac{pr}{\sqrt{4t_r^2 - p^2r^2}} \qquad [21]$$

so that Equation [20] becomes

$$\epsilon_r = \epsilon_\theta + r\frac{d\epsilon_\theta}{dr} + \frac{1}{2}\frac{p^2r^2}{4t_r^2 - p^2r^2} \qquad [22]$$

Equations [10] and [19] imply

$$\frac{t_r}{t_\theta} = \frac{2\epsilon_r + \epsilon_\theta}{2\epsilon_\theta + \epsilon_r} \qquad [23]$$

or, by Equation [18]

$$t_r(2\epsilon_\theta + \epsilon_r) = \left[t_r + r\frac{d(t_r)}{dr}\right](2\epsilon_r + \epsilon_\theta)$$

Thus

$$t_r(\epsilon_\theta - \epsilon_r) = r\frac{d(t_r)}{dr}(2\epsilon_r + \epsilon_\theta)$$

or

$$\frac{d(t_r)}{dr} = \frac{\epsilon_\theta - \epsilon_r}{2\epsilon_r + \epsilon_\theta}\frac{t_r}{r} \qquad [24]$$

From Equation [10a] and Equations [16] and [19] there follows

$$t_r = h_0 2\frac{\tau(\gamma)}{\gamma}(2\epsilon_r + \epsilon_\theta)(1 - \epsilon_r - \epsilon_\theta) \qquad [25]$$

Equations [22], [24], [25], and [11], are four equations in the four variables ϵ_r, ϵ_θ, γ, and t_r. Inspection shows that they are equivalent to a

single second-order differential equation in one dependent variable, say ϵ_θ. There will consequently be two arbitrary constants of integration. These constants will be determined by two boundary conditions, for example, $\epsilon_\theta(a) = 0$, $\epsilon_\theta(-a) = 0$, where a is the prescribed radius of the plate. The solutions of these equations and Equation [21] will depend not only on the radius a, but also on the two arbitrary parameters p and h_0. Fortunately, the triple infinity of solutions resulting may easily be obtained from a single infinity of solutions depending on only one parameter pa/h_0. To verify this statement it is necessary merely to rewrite Equations [21], [22], [24], [25], and [11] in the form

$$\frac{d\left(\frac{z}{a}\right)}{d\left(\frac{r}{a}\right)} = \frac{\left(\frac{pa}{h_0}\right)\left(\frac{r}{a}\right)}{\sqrt{4\left(\frac{t_r}{h_0}\right)^2 - \left(\frac{pa}{h_0}\right)^2\left(\frac{r}{a}\right)^2}}$$

$$\epsilon_r = \epsilon_\theta + \frac{r}{a}\frac{d\epsilon_\theta}{d\left(\frac{r}{a}\right)} + \frac{1}{2}\,\frac{\left(\frac{pa}{h_0}\right)^2\left(\frac{r}{a}\right)^2}{4\left(\frac{t_r}{h_0}\right)^2 - \left(\frac{pa}{h_0}\right)^2\left(\frac{r}{a}\right)^2}$$

$$\frac{d\left(\frac{t_r}{h_0}\right)}{d\left(\frac{r}{a}\right)} = \frac{1}{\frac{r}{a}}\,\frac{t_r}{h_0}\,\frac{\epsilon_\theta - \epsilon_r}{2\epsilon_r + \epsilon_\theta}$$

$$\frac{t_r}{h_0} = 2\,\frac{\tau(\gamma)}{\gamma}(2\epsilon_r + \epsilon_\theta)(1 - \epsilon_r - \epsilon_\theta)$$

$$\gamma = 2\sqrt{\frac{2}{3}}\,\sqrt{(\epsilon_r^2 + \epsilon_r\epsilon_\theta + \epsilon_\theta^2)}$$

In the foregoing equations r/a is the independent variable, and the dependent variables are now z/a, ϵ_r, ϵ_θ, γ, and t_r/h_0, the parameter being pa/h_0. The two boundary conditions are that $\epsilon_\theta = 0$ when $\frac{r}{a} = \pm 1$. Although the existence of these "proportionate coordinates" has now been established, it is convenient to continue the analysis with the original coordinates. Only the graphs of the solutions need be given in proportionate units.

After the functions $\epsilon_r(r)$, $\epsilon_\theta(r)$, and $t_r(r)$ have been determined by solving Equations [22], [24], [25], and [11], the deflection function $z(r)$ will be found by integrating Equation [21]; the constant of integration is fixed by the boundary condition $z = 0$ when $r = a$. The quantities such as t_θ, σ_r, σ_θ, u, and h may also be computed by Equations [10], [11], [15], [16], [17], [18], and [19].

It is convenient to plot t_r/h_0 as a function of ϵ_r and ϵ_θ, using Equations [11] and [25]. Figure 7 is such a graph, in which $\tau(\gamma)$ is taken as in Figure 3, which in turn was based on the tensile test curve of Figure 2. Figure 7 may be considered to describe the biaxial stress-strain properties of a thin plate of the material.

NUMERICAL SOLUTION OF EQUATIONS [11], [21], [22], [24], [25]

Equations [24] and [22] are equivalent to

$$t_r = t_0 - \int_0^r \frac{t_r}{r} \frac{\epsilon_r - \epsilon_\theta}{2\epsilon_r + \epsilon_\theta} \, dr \qquad [26a]$$

$$\epsilon_\theta = \epsilon_0 - \int_0^r \left(\frac{1}{2} \frac{p^2 r}{4t_r^2 - p^2 r^2} - \frac{\epsilon_r - \epsilon_\theta}{r} \right) dr \qquad [26b]$$

where t_0 is the value of the tension t_r at $r = 0$ and ϵ_0 is the value of the strain ϵ_θ at $r = 0$.

Equations [26] are solvable numerically by iteration of the two integrals, by the use of Equations [11] and [25], as follows: Suppose approximations for t_r and ϵ_θ in terms of r are known. Then Equations [11] and [25], or the graph of Figure 7, give ϵ_r in terms of r. Substituting these approximations of t_r, ϵ_θ, and ϵ_r in the right-hand side of Equations [26] and integrating, we obtain new approximations for t_r and ϵ_θ. The process may then be repeated indefinitely. A measure of the accuracy of a solution is its proximity to the previous one.

When sufficiently accurate evaluations of ϵ_r and ϵ_θ have been secured, Equations [10] may be used to find σ_r and σ_θ.

Finally, the deflection function $z(r)$ may be evaluated by an integration, since by solving for z in Equation [21], there results

$$z = z_0 - \int_0^r \frac{pr}{\sqrt{4t_r^2 - p^2 r^2}} \, dr$$

where z_0 is evaluated so that $z(a) = 0$. Then z_0 is the calculated central deflection of the plate.

CHOICE OF PARAMETERS

A number of details concerned with the process of the numerical solution are of interest. It has been seen that there are but three independent parameters. Hence only three of the six quantities z_0, t_0, ϵ_0, h_0, p, and a may be chosen in advance. Thus, for example, the thickness and radius of a

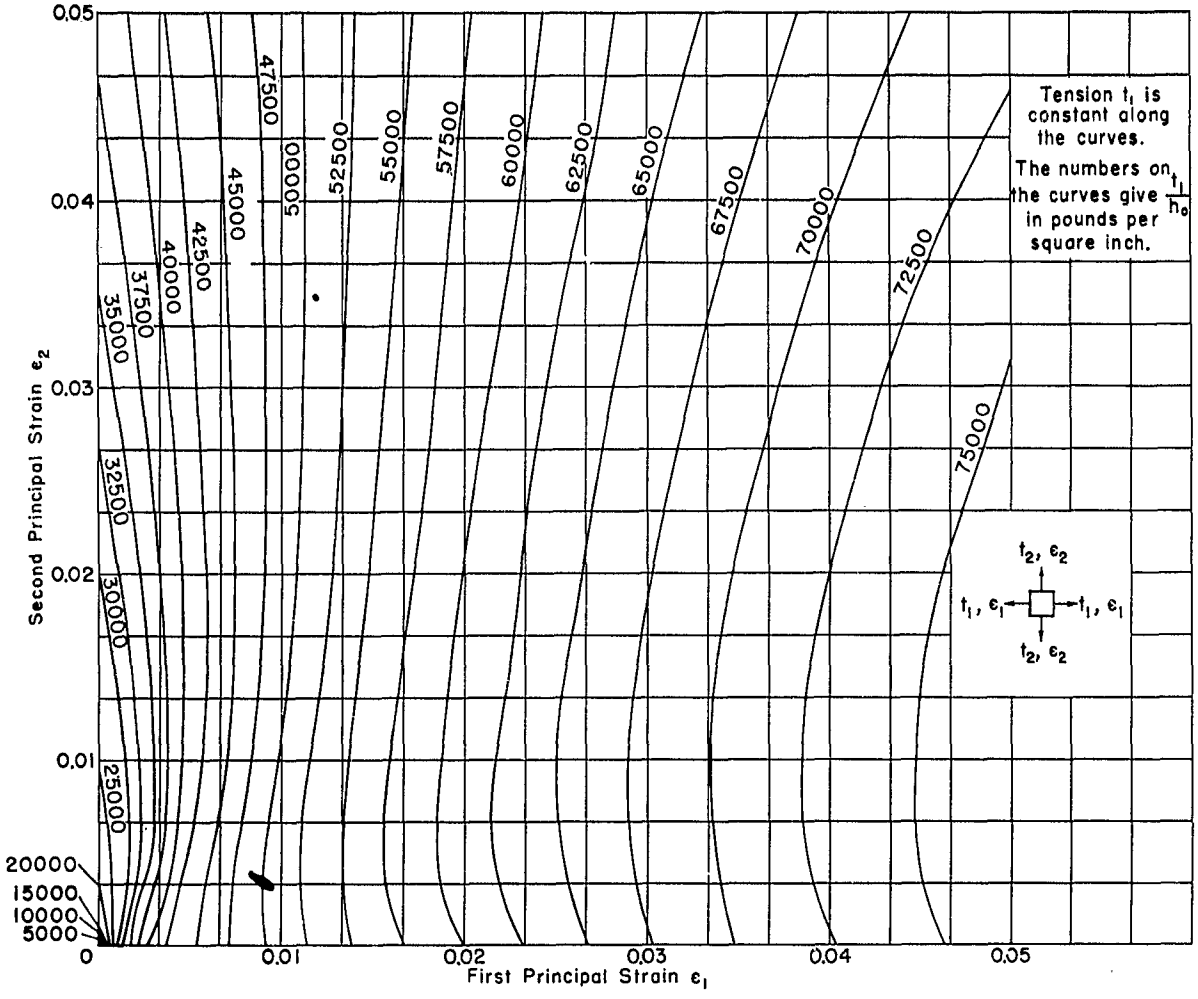

Figure 7 - Tension Due to Biaxial Strain

Let ϵ_1 and ϵ_2 be the principal strains in the plane of a thin plate and let t_1 and t_2 be the corresponding principal tensions. The curves shown here are curves of constant t_1/h_0 plotted on ϵ_1 and ϵ_2.

The quantity t_1/h_0 corresponding to ϵ_1 and ϵ_2 was computed by the formulas

$$\frac{t_1}{h_0} = 2\,\frac{\tau(\gamma)}{\gamma}(2\epsilon_1 + \epsilon_2)(1 - \epsilon_1 - \epsilon_2)$$

$$\gamma = 2\sqrt{\frac{2}{3}}\,\sqrt{\epsilon_1^2 + \epsilon_1\epsilon_2 + \epsilon_2^2}$$

The function $\tau(\gamma)$ was taken to be the curve of Figure 3 obtained from the tensile-test curve on a medium-steel specimen shown in Figure 2; see pages 6 and 7 respectively.

If any two of the three quantities t_1/h_0, ϵ_1, and ϵ_2 are given, the third quantity may be found by interpolation on the graph.

This graph, where we have taken $\epsilon_r = \epsilon_1$, $t_r = t_1$, and $\epsilon_\theta = \epsilon_2$, was used to find ϵ_r in the theoretical computations from t_r and ϵ_θ.

plate may be given and the deflection and strains may be sought as functions of the pressure applied. Or, in other instances, the radius of a plate and its central deflection at a given pressure may be fixed and the thickness required to obtain this central deflection may be sought.

The numerical solution may be more lengthy with some choices of parameters than with others. If p, h_0, and ϵ_0 are given, the procedure is simpler than, for example, when p, h_0, and a are given, for t_0 can be computed from ϵ_0 and h_0 by Equation [25] and each integration of Equations [26] gives a better approximation of t_r and ϵ_θ. When t_r and ϵ_θ have been determined with a sufficient degree of accuracy as functions of r, the radius of the plate is determined by setting ϵ_θ equal to zero and solving for r. This value of r is the radius a. The deflection z is then found by integration using Equation [21], and z_0 is determined so that $z(a) = 0$. If, instead, p, h_0, and the radius a of the plate are considered known, estimates are first made for z_0, ϵ_0, t_0.* Then Equations [26], [25], and [11] are used iteratively to find sufficiently accurate determinations of t_r and ϵ_θ, and a calculated radius of the plate a' is obtained by setting ϵ_θ equal to zero. On the basis of these results new evaluations of z_0, ϵ_0, and t_0 are made and the process is repeated until a' is sufficiently close to the given radius a of the plate. In the case where a family of solution curves is desired, it is equally effective and more direct to proceed by the first method, selecting suitable sets of values for p, h_0, and ϵ_0.

FIRST APPROXIMATIONS

To facilitate the choice of first approximations for ϵ_θ, t_r, etc., the following formulas are set down. Experiments show that a deflected plate is approximately a spherical cap. Consequently the tensions t_θ and t_r are approximately equal and constant throughout the plate. That is, the relationship

$$t_r \approx t_\theta \approx t_0$$

where t_0 is the common tension at the center, is approximately true for all radial values r. It then follows from Equation [23] that

$$\epsilon_r \approx \epsilon_\theta$$

A first-order approximation to a spherical deflection function is the parabolic deflection function vanishing at $r = a$:

$$z = z_0\left(1 - \frac{r^2}{a^2}\right) \qquad [27]$$

* Estimates may be made from formulas given in the next section.

where z_0 is the deflection at $r = 0$

It may be shown (14) that, for a membrane of tension t_0, p is given precisely by

$$p = \frac{4t_0 z_0}{a^2 + z_0^2}$$

This form is preferable when z_0 is large compared to a.

Experiments show that ϵ_θ varies in an approximately parabolic manner. Hence, as a first approximation

$$\epsilon_\theta = \epsilon_0\left(1 - \frac{r^2}{a^2}\right)$$

where ϵ_0 is the strain at the center.

The quantity t_0/h_0 can be calculated when ϵ_0 is pre-assigned. For at $r = 0$, $\epsilon_r = \epsilon_\theta = \epsilon_0$, and Equation [25] reduces to

$$\frac{t_0}{h_0} = 6\frac{\tau(\gamma_0)}{\gamma_0}\epsilon_0(1 - 2\epsilon_0)$$

where γ_0 is the value of γ at $r = 0$. By Equation [11]

$$\gamma_0 = 2\sqrt{2\epsilon_0}$$

and

$$\frac{t_0}{h_0} = \frac{3}{\sqrt{2}}\tau(\gamma_0)(1 - 2\epsilon_0)$$

Finally, there may be written the approximate law

$$\epsilon_0 = \frac{z_0^2}{a^2}$$

The plausibility of this relationship may be demonstrated as follows. Combining Equation [16] and the approximate equations $\epsilon_r = \epsilon_\theta = \epsilon_0(1 - r^2/a^2)$ which were found in the foregoing, we obtain

$$h_0 - h = 2\epsilon_0 h_0\left(1 - \frac{r^2}{a^2}\right)$$

i.e., a parabolic variation of $h_0 - h$ is implied. The volume V of the plate before deformation is equal to its volume after deformation. Hence,

$$V = \int_0^a 2\pi r\sqrt{1 + \left(\frac{dz}{dr}\right)^2}\, h_0\left[1 - 2\epsilon_0\left(1 - \frac{r^2}{a^2}\right)\right]dr$$

$$= \pi a^2 h_0$$

Therefore, to a first approximation

$$\int_0^a 2r\left[1 + \frac{1}{2}\left(\frac{dz}{dr}\right)^2\right]\left[1 - 2\epsilon_0\left(1 - \frac{r^2}{a^2}\right)\right]dr = a^2$$

Since

$$z = z_0\left(1 - \frac{r^2}{a^2}\right)$$

and

$$\left(\frac{dz}{dr}\right)^2 = \frac{4r^2z_0^2}{a^4}$$

it follows that

$$\int_0^a\left[2r + \frac{4r^3z_0^2}{a^4}\right]\left[1 - 2\epsilon_0\left(1 - \frac{r^2}{a^2}\right)\right]dr = a^2$$

or

$$\int_0^a\left\{2r + \frac{4r^3z_0^2}{a^4} - 4\epsilon_0 r\left(1 - \frac{r^2}{a^2}\right) - \frac{4r^3z_0^2}{a^4}\left[2\epsilon_0\left(1 - \frac{r^2}{a^2}\right)\right]\right\}dr = a^2$$

We may neglect the term $\frac{4r^3z_0^2}{a^4}\left[2\epsilon_0\left(1 - \frac{r^2}{a^2}\right)\right]$ since it is small relative to the others. The equation may then be reduced to

$$\int_0^a\left[\frac{4r^3z_0^2}{a^4} - 4\epsilon_0 r\left(1 - \frac{r^2}{a^2}\right)\right]dr = 0$$

Finally,

$$z_0^2 = 4\epsilon_0\left(\frac{a^2}{2} - \frac{a^2}{4}\right)$$

or

$$\epsilon_0 = \frac{z_0^2}{a^2}$$

For convenience the foregoing approximate formulas are rewritten in collected form

$$\left.\begin{aligned} \epsilon_0 &= \frac{z_0^2}{a^2} \\ p &= \frac{4t_0z_0}{a^2 + z_0^2} = \frac{4t_0\sqrt{\epsilon_0}}{a(1 + \epsilon_0)} \end{aligned}\right\} \qquad [28]$$

$$\left.\begin{aligned} \frac{t_0}{h_0} &= \frac{3}{\sqrt{2}}\,\tau(\gamma_0)(1 - 2\epsilon_0) \\ \gamma_0 &= 2\sqrt{2\epsilon_0} \end{aligned}\right\} \qquad [28]$$

$$\left.\begin{aligned} t_r &= t_\theta = t_0 \\ z &= z_0\left(1 - \frac{r^2}{a^2}\right) \\ \epsilon_\theta &= \epsilon_r = \epsilon_0\left(1 - \frac{r^2}{a^2}\right) \end{aligned}\right\} \qquad [29]$$

Equations [28] give four independent relations among the seven quantities t_0, z_0, ϵ_0, h_0, p, a, and γ_0. Hence, if any three of these seven quantities are given, the others may be determined if $\tau(\gamma)$ is known. The successive approximations furnished by Equations [26], [25], and [11] may then be determined, starting with the evaluations for t_r and ϵ_θ based on Equations [29].

This completes the consideration of initial approximations for use in Equations [26], [25], and [11].

APPLICATION OF THE METHOD

The methods discussed in the foregoing for predicting the action of a circular clamped plate under pressure will now be applied. The material selected to show the application of the method is medium steel having the $\tau(\gamma)$ characteristic of Figure 3 for the tensile specimen with the stress-strain curve of Figure 2; see pages 6 and 7 respectively. For the purposes of starting the computations a nominal radius of 10 inches and a thickness of 1/8 inch were chosen and used in the initial formulas. The results as finally presented in Figures 8 to 12 inclusive are in terms of the general parameters discussed on page 15, and so apply to any thin plate with a similar $\tau(\gamma)$ characteristic.

The first step in the computation is to select a range of values of z_0 and substitute them and the chosen values of h_0, a, and $\tau(\gamma)$ in the approximate formulas, Equations [28], to obtain a table such as Table 1.

The second step in the computation is to tabulate t_r and ϵ_θ for selected values of radial distance, using the first and third of Equations [29]. The values of ϵ_0, t_0, and p in Table 1 are now to be considered exact and will be used throughout the remaining computations. The values of a and z_0 used thus far are entirely discarded from this point on. They served merely as a convenience for starting the calculations. New and exact values

TABLE 1

Approximate Values of ϵ_0, t_0, and p

The radius a is taken to be 10 inches and h_0 to be 1/8 inch.

z_0 in inches	$\epsilon_0 = \frac{z_0^2}{a^2}$	$t_0 = \frac{3}{\sqrt{2}} h_0 \tau(\gamma_0)(1 - 2\epsilon_0)$ in pounds per inch	$p = \frac{4 t_0 z_0}{a^2 + z_0^2}$ in pounds per square inch
0.2	0.0004	3206	25.64
0.5	0.0025	4670	93.17
1.0	0.01	6289	251.56
1.5	0.0225	7510	416.5
2.0	0.04	8738	699.00
2.5	0.0625	9334	878.5
3.0	0.09	9528	1049.00

of z_0 and a will later be determined for each set of values ϵ_0, t_0, and p. The third step is the graphical determination from Figure 7 of ϵ_r corresponding to the values of t_r and ϵ_θ tabulated in Step 2. The fourth step is to substitute these evaluations of t_r, ϵ_θ, and ϵ_r in the integration formulas [26] to secure new values of t_r and ϵ_θ by numerical integration. Steps 3 and 4 are then repeated until successive approximations of t_r, ϵ_θ, and ϵ_r show little change. If now the values of ϵ_θ for a set of values ϵ_0, t_0, h_0, and p from Table 1 are plotted against radial distance, it will be found that ϵ_θ becomes zero at a radial distance which is found to approximate 10 inches, the value used to obtain Table 1. The radial distance at which ϵ_θ is zero must be considered the exact value of the radius a corresponding to the set ϵ_0, t_0, and p. This value of a is used, of course, in computing quantities such as r/a and pa/h_0 for this set. Similarly other values of a approximating 10 inches will be found for other sets of ϵ_0, t_0, and p. The quantities ϵ_r and ϵ_θ were computed in this manner and the results are plotted for the various sets as shown in Figures 8 and 9.

Other quantities such as t_θ, σ_r, and σ_θ may readily be calculated by means of Equations [23], [16], and [19]. The quantities σ_r and σ_θ were determined in this manner and the results are shown in Figures 10 and 11.

The deflection z at radial distance r may be computed by Equation [21]. The values of z_0 thus obtained, which differ somewhat from those used in Table 1, are the exact values of central deflection corresponding to the

(Text continued on page 27)

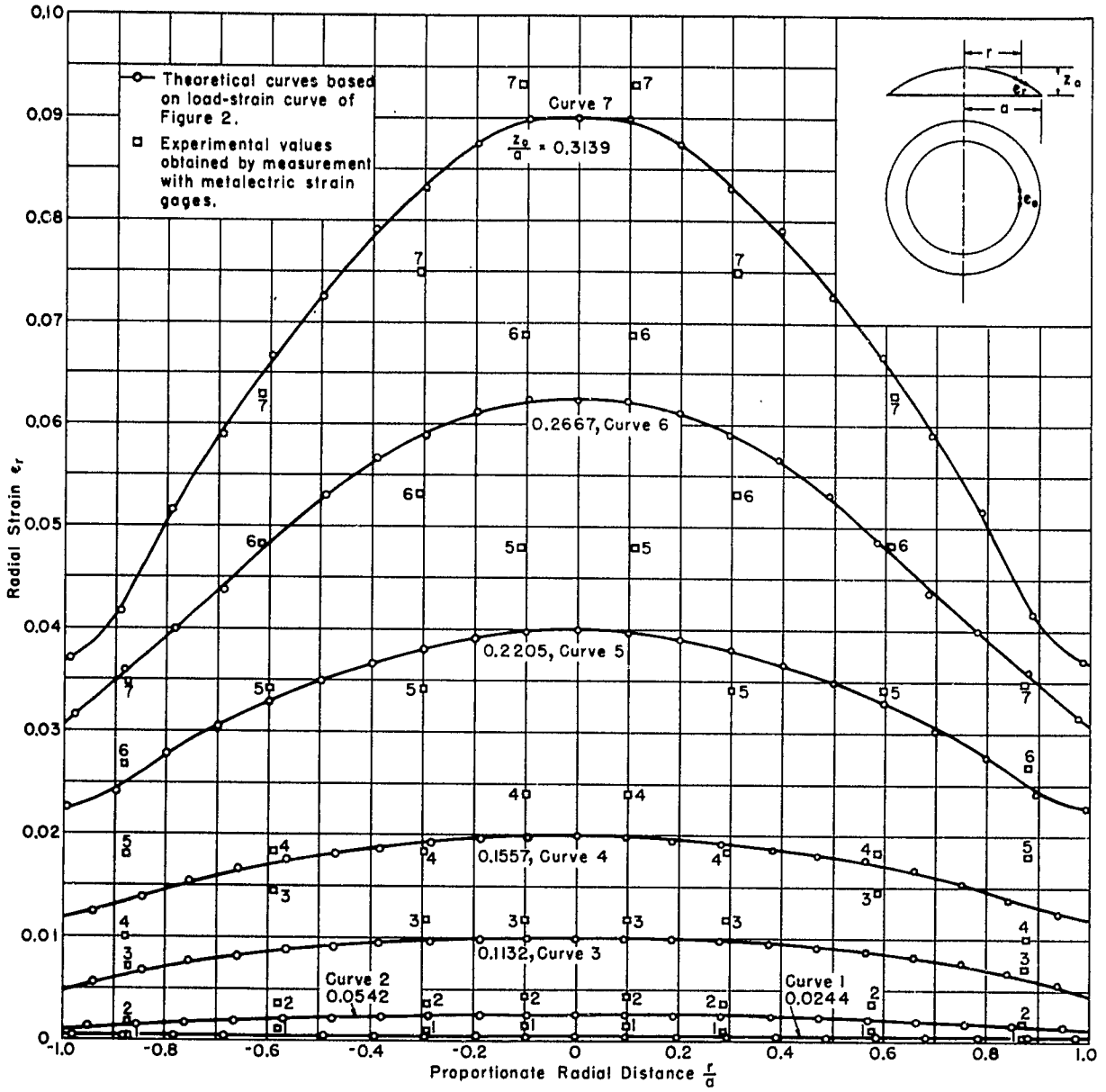

Figure 8 - Radial Strain Plotted against Radial Distance

Radial strains were computed by integration of equilibrium conditions, strain-displacement relations, and stress-strain equations of plasticity. The load-strain curve of Figure 2, taken from a tensile test on a specimen of the same material as the plate, medium steel, was employed.

Experimental points numbered 1 to 7 are to be compared with points on the theoretical curves 1 to 7 respectively.

It should be noted that in this set of curves z_0/a was used as the parameter instead of pa/h_0.

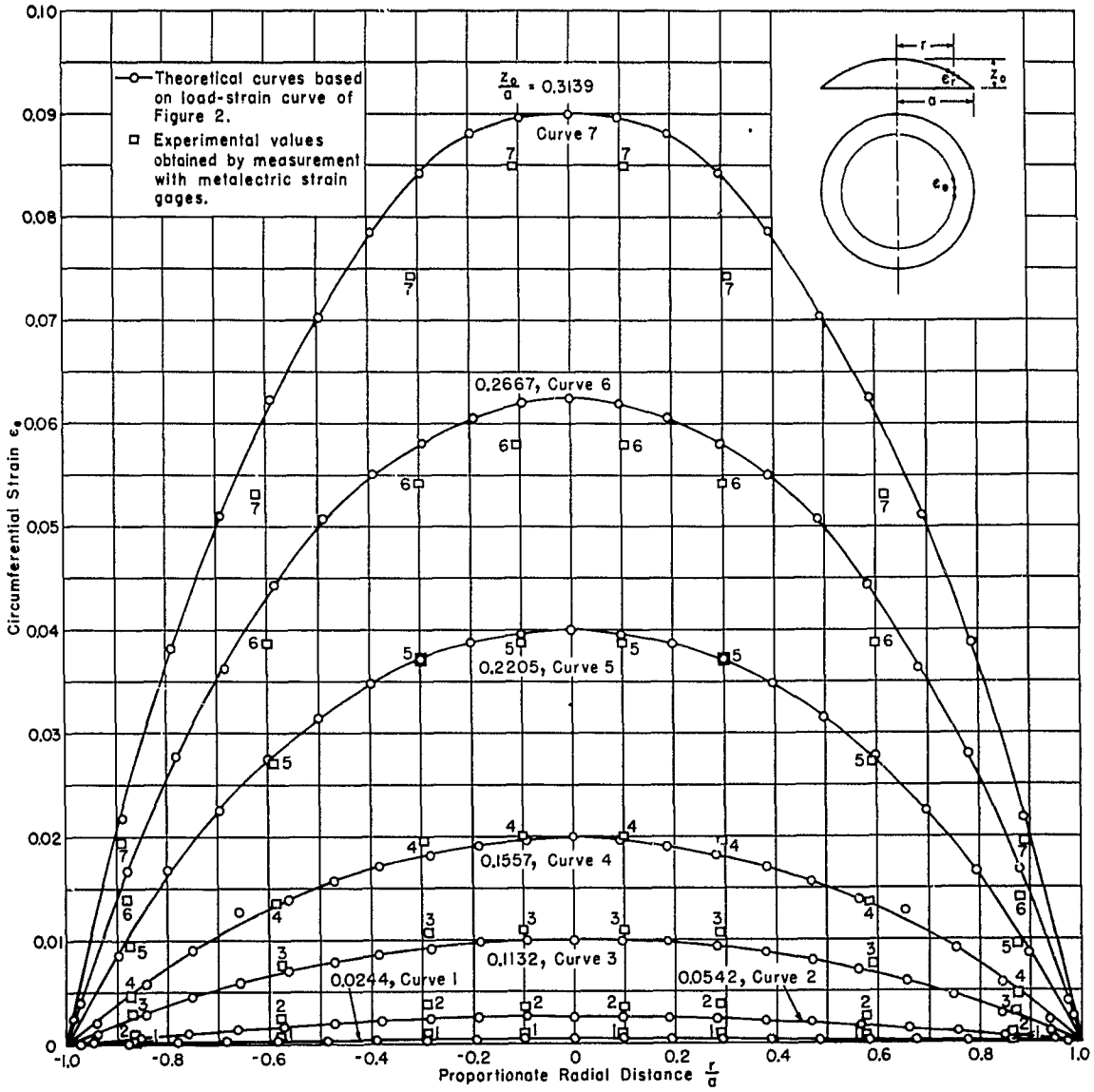

Figure 9 - Circumferential Strain Plotted against Radial Distance

Circumferential strains were computed by integration of equilibrium conditions, strain-displacement relations, and stress-strain equations of plasticity. The load-strain curve of Figure 2 obtained from a tensile test on a specimen taken from the same material as the plate, medium steel, was employed; see page 6.

Experimental points numbered 1 to 7 are to be compared with points on the theoretical curve 1 to 7, respectively.

It should be noted that in this set of curves z_0/a was used as the parameter instead of pa/h_0.

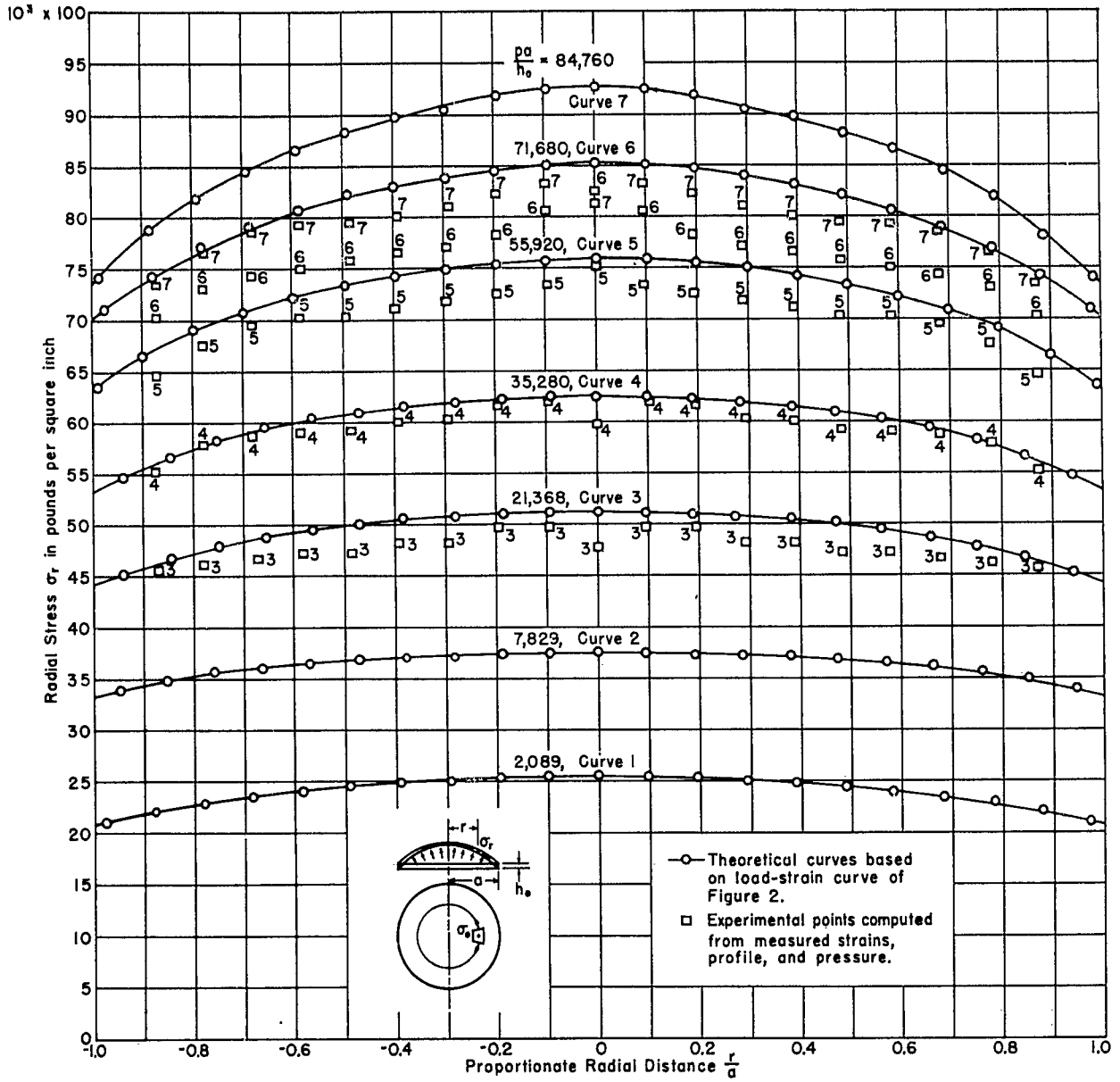

Figure 10 - Radial Stress Plotted against Radial Distance

Radial stresses in a thin circular plate were computed by integration of equilibrium, strain-displacement, and plasticity laws. The load-strain curve of Figure 2 obtained from a tensile test on a specimen taken from the same material as the experimental plate, medium steel, was employed.

Experimental points numbered 3 to 7 are to be compared with points on the theoretical curves 3 to 7, respectively.

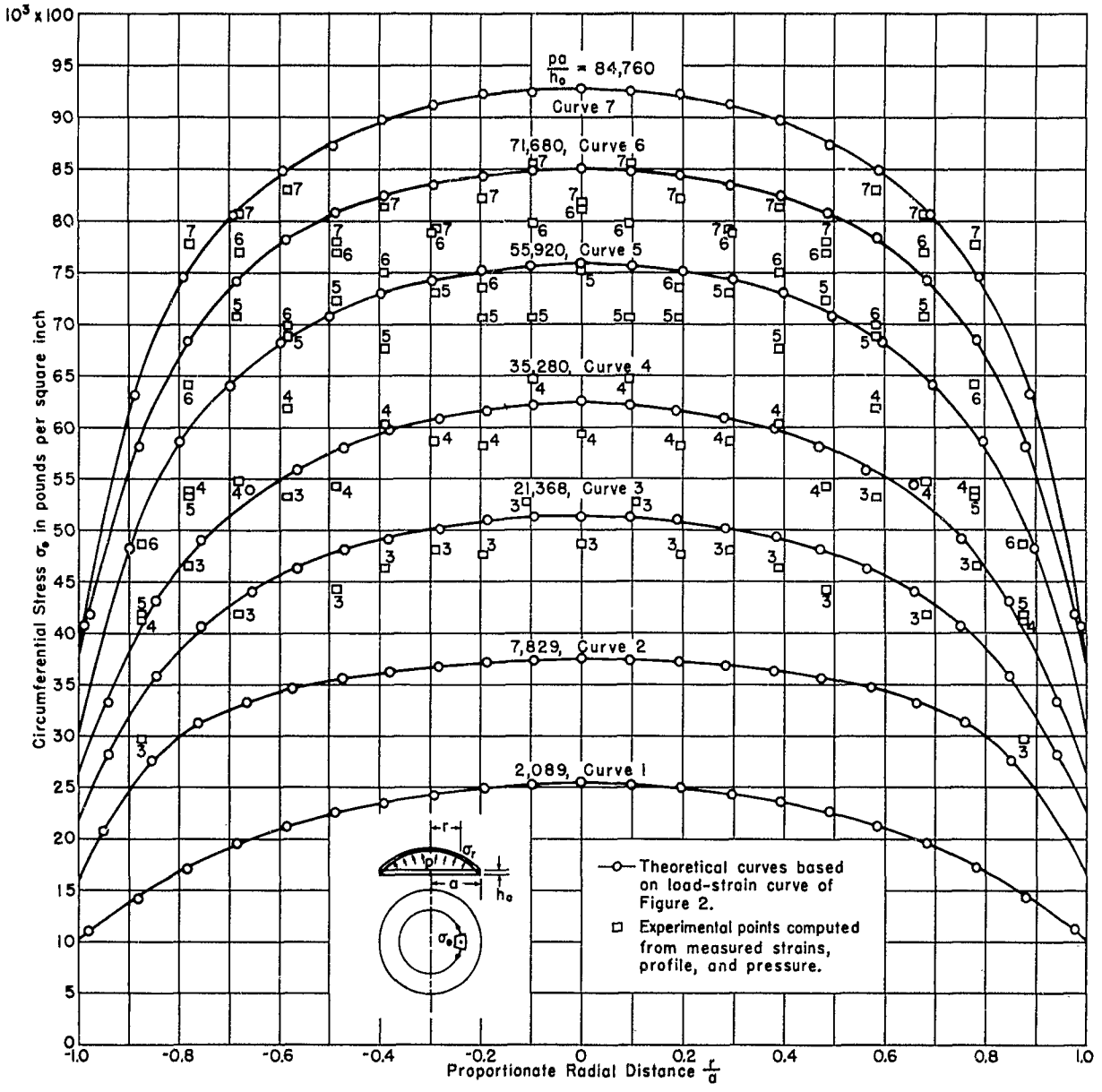

Figure 11 - Circumferential Stress Plotted on Radial Distance

Circumferential stresses were computed for a thin circular plate by integration of equilibrium, strain-displacement, and plasticity laws. The load-strain curve of Figure 2 obtained from a tensile test on a specimen taken from the same material as the experimental plate, medium steel, was employed; see page 6.

Experimental points numbered 3 to 7 are to be compared with points on the theoretical curves 3 to 7, respectively.

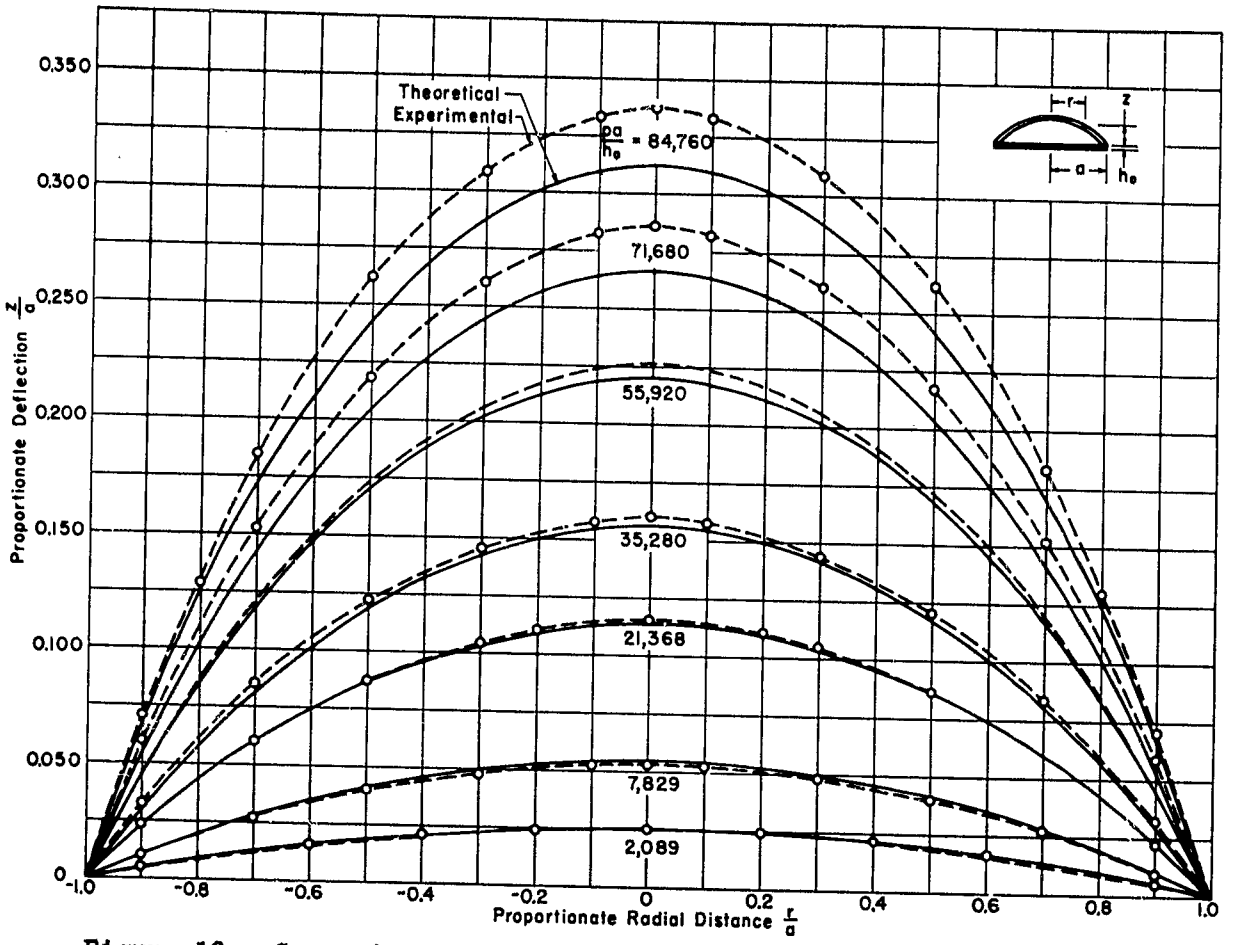

Figure 12 - Comparison of Theoretical and Experimental Profile Curves at Corresponding Pressures for a Plate of Medium Steel

The theoretical deflection curves shown here were obtained by solution of the equilibrium conditions, strain-displacement relations, and the plastic stress-strain laws.

The 8 per cent discrepancy in center deflection can be ascribed chiefly to the fact the $\tau(\gamma)$ curve obtained from a tensile test on a specimen gave values of τ for biaxial stresses about 8 per cent too high; see Figure 3 on page 7.

sets ϵ_0, t_0, and p. Figure 12 shows curves of deflection plotted against radial distance for various pressures thus obtained.

Figures 8, 9, 10, 11, and 12 are plotted by use of the proportionate coordinates introduced and established by the equations on page 15. The figures therefore apply to any thin circular plate of material with the $\tau(\gamma)$ characteristic of Figure 3, as given on page 7.

COMPARISON OF THEORY AND EXPERIMENT

With each of the graphs for ϵ_r, ϵ_θ, σ_r, σ_θ, and z computed as in the foregoing are shown corresponding experimental points. The data from which these experimental points were taken were obtained at the Taylor Model

Basin (15) on a circular medium-steel plate nominally 20 inches in diameter and 1/8 inch thick. This plate was machined from the same stock as the tensile specimen which yielded the $\tau(\gamma)$ curve used in the calculations of this report. The fact that in the tests the rim bounding the plate had a curved edge of 1/2-inch radius, as in Figure 1, made necessary a correction to the plate radius. In the computations of the experimental data a value of 10.25 inches was assumed as the radius a.

As the test plate was deformed under pressure, measurements were made of the deflection z and the strains ϵ_θ and ϵ_r at selected radii. From these data and Equations [16], [17], [18], and [19] the values of σ_r and σ_θ were computed and plotted as the experimentally determined points.

The deflection curves of Figures 12 and 13 are considered to be the most significant check of theory and experiment in that the deflection is subject to direct observation with only small error. The two sets of curves in Figures 12 and 13 correspond in pairs to selected values of the proportionate pressure pa/h_0. It will be seen that at low pressures the agreement is within a few per cent. As the pressure is increased, the experimental values exceed

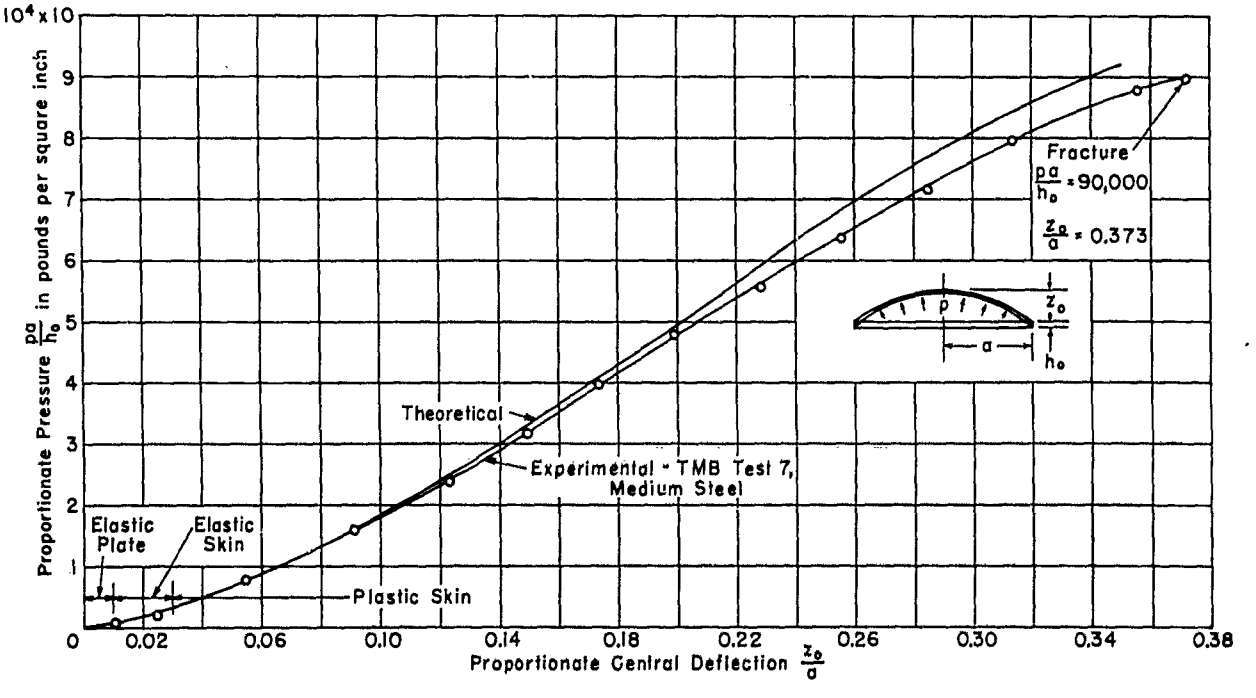

Figure 13 - Comparison of Theoretical and Experimental Curves of Pressure against Center Deflection

The theoretical curve was obtained by integration of equilibrium, strain-displacement, and plasticity laws using a load-strain curve obtained from a medium-steel specimen.

The experimental curve was obtained by direct measurement on a medium-steel plate of nominal radius 10 inches and thickness 1/8 inch.

the calculated values by larger amounts; the largest discrepancy is about 8 per cent.

The lower of the two $\tau(\gamma)$ curves in Figure 3 on page 7 was obtained from the experimental stresses and strains for the center of the plate, by the use of Equations [2] and [11]. This curve may be referred to as the experimental $\tau(\gamma)$ curve for the plate. The other curve shown in Figure 3, although obtained experimentally from a uniaxial test, may conveniently be regarded as the *theoretical* $\tau(\gamma)$ curve for the plate. It will be noted that the theoretical values of τ exceed the experimental ones for a given value of γ. Because of high theoretical values of τ, theoretical stresses should be high for a given pair of strains. This statement is corroborated by the stress values shown in Figures 10 and 11. As expected, the theoretical values of stress are generally higher than the experimental ones for a given value of pa/h_0; at high pressures the difference may be as much as 10 per cent. As a result of high theoretical stresses, the theoretical pressure is high for a given deflection. It follows that the theoretical deflections should be lower than the experimental ones for a given pressure. These deductions are also corroborated by the deflection curves of Figures 12 and 13.

In Figures 8 and 9 on pages 23 and 24 the theoretical and experimental values of strain are presented for selected values of z_0/a. It is believed that a major portion of the discrepancy between theoretical and experimental values of strain may be ascribed to errors arising from difficulties encountered in using metalectric strain gages. It will be seen that at low deflections the theoretical values of strain usually are exceeded by the computed values. The measured values exceed estimates based on any of the known plate or membrane formulas for small or moderate deflections. As the deflection is increased, there is agreement on the average in Figure 8 except at large values of radial distance. A small portion of the discrepancy near the edge of the plate may be due to bending strains since such strains were not taken into account in the theory. In this region the experimental plate should be less convex than the theory indicates, and the measured radial strains accordingly less for a given value of z_0/a.

Computations not described in this report show that a better check of theoretical and experimental values of deflection will result if logarithmic strains are used in place of the conventional strains in the assumed plasticity laws. Such a refinement and the elimination of the discrepancy between uniaxial and biaxial $\tau(\gamma)$ characteristics obtained in the tests are believed generally to outweigh other refinements that could be made in the theory, such as the inclusion of bending stresses or the use of exact strain-displacement relations in the computations in place of first-order approximations.

CONCLUSIONS

The plasticity laws, Equations [1] and [2], together with equilibrium conditions and strain-displacement relationships for the clamped, thin, circular plate under pressure, may be numerically integrated to give theoretical values of stresses, strains, and deflections at a given pressure.

Results so obtained were found to be in agreement with experiment within about 10 per cent.

REFERENCES

(1) "Über den Spannungszustand in kreisrunden Platten mit verschwindender Biegungsteifigkeit" (The Stress Condition in Circular Plates with Infinitely Small Bending Strength), by H. Hencky, Zeitschrift für Mathematik und Physik, Vol. 63, 1915, p. 311.

(2) "Bending of Circular Plates with Large Deflections," by S. Way, Transactions of the American Society of Mechanical Engineers, Vol. 56, 1934, p. 627.

(3) "Elemente der Technologischen Mechanik" (Elements of Technological Mechanics), by P. Ludwik, Springer, Berlin, 1909.

(4) "The Intrinsic Theory of Elastic Shells and Plates," by J.L. Synge and W.Z. Chien, Theodore von Kármán Anniversary Volume, p. 103.

(5) "Plasticity," by A. Nadai, McGraw-Hill, New York, N.Y., 1931.

(6) "Plastic Behavior of Metals in the Strain Hardening Range," by A. Nadai, Journal of Applied Physics, Vol. 8, 1937, p. 205.

(7) "Mechanik der festen Körper im plastisch deformablen Zustand" (Mechanics of Solids in a Condition of Plastic Deformability), by R. von Mises, Göttinger Nachrichten, 1913.

(8) "Abhandlungen aus dem Gebiete der Technischen Mechanik" (Treatises in the Field of Technical Mechanics), by O. Mohr, Ernst U. Sohn, Berlin, Second Edition, 1914.

(9) "The Failure of Diaphragms under Uniform Pressure," by Merit P. White, National Defense Research Committee, Armor and Ordnance Report A-167, April 1943.

(10) "Über den Zusammenhang von Spannungen und Formänderungen im Verfestigungsgebiet" (On the Relation of Stresses and Deformations in the Range of Work Hardening), by R. Schmidt, Ingenieur-Archiv, Vol. III, 1932, p. 215.

(11) "Theories of Strength," by A. Nadai, Transactions of the American Society of Mechanical Engineers, APM-55-15, 1933, p. 111.

(12) "Plastic Behavior of Metals in the Strain Hardening Range," by E.A. Davis, Part II, Journal of Applied Physics, Vol. 8, 1937.

(13) "The Increase of Stress with Permanent Strain and the Stress-Strain Relations in the Plastic State for Copper under Combined Stresses," by E.A. Davis, Westinghouse Research Laboratories, Scientific Paper 1115, June 1943.

(14) "Protection against Underwater Explosion - Plastic Deformation of a Circular Plate," by A.N. Gleyzal, TMB Report 490, September 1942.

(15) "Plastic Strain and Deflection Tests on Clamped Circular Steel Plates 20 Inches in Diameter," by A.N. Gleyzal, TMB Report R-142, May 1944.